IONIZATION MEASUREMENT IN A STREAMER CHAMBER

T. L. Asatiani, K. A. Gazaryan, V. A. Ivanov, V. N. Zhmyrov, and A. A. Nazaryan
Joint Institute for Nuclear Research; Physics Institute, Erevan
Submitted 15 January 1967; resubmitted 16 June 1967
ZhETF Pis'ma 6, No. 4, 571-575 (15 August 1967)

Unlike in a cascade chamber [3], in a streamer chamber the number of glowing centers is a saturable parameter and cannot be used to measure ionization. As shown by Chikovani et al. [2], a more convenient parameter for the measurement of ionization in a streamer chamber should be the brightness of the ionizing-particle track. In fact, the total time τ in which the particle track is produced consists of the time τ_{cr} needed for the cascade develop to its critical dimension and the streamer growth time τ_{st}: $\tau = \tau_{cr} + \tau_{st}$.

Usually τ_{cr} is equal to 10 - 40 nsec, depending on the operating conditions of the streamer chamber, and τ_{st} does not exceed several nanoseconds. Therefore a slight change of τ_{st} leads to a noticeable change in the brightness of the streamer track. The time of growth of the cascade to the critical dimension decreases with increasing primary ionization. At a fixed duration of the high-voltage pulse, this leads to an increase in the growth time of the streamer column, and consequently to a growth in the brightness of the streamer track.

We present in this paper the results of an experiment aimed at investigating the possibility of measuring the ionizing ability of charged particles in a streamer chamber.

A streamer chamber measuring 50 x 35 x 15 cm, filled in one case with pure neon and in the other with commercial helium, was irradiated by a beam of protons of different energies (JINR synchrocyclotron). A high-voltage pulse generated by an ordinary Marx generator was fed to the chamber electrodes, in the presence of triple coincidences of the scintillation-telescope counters. The amplitude of the high-voltage pulse was approximately 150 kV. The pulse duration was varied by changing the length of the shunting discharge gap, thereby essentially changing the streamer growth time τ_{st}.

Three series of measurements were made (I, II, III) at three times of streamer-track formation, corresponding to streamer lengths 6 - 11 mm in neon at a proton energy 660 MeV (τ_I = 40 nsec, τ_{II} and τ_{III} longer by 1 - 3 nsec respectively). One series of measurements was made with helium at a streamer length $\sim$ 20 mm.

In each measurement series, at a fixed duration of the high-frequency pulse, we photographed the tracks of protons of different energies traveling perpendicular to the direction of the electric field.* The photographs were taken along the electric field (projection A) and perpendicular to the field (projection B). The photographs revealed clearly the growth of the streamer columns (projection B) and the increase in the brightness of the proton tracks (projection A) with increasing ionizing ability. Reduction of the photographs yielded the following parameters: (a) the average streamer length $\bar{l}$ for the tracks of protons having the same energy, by determining the widths of the individual tracks (projection B) and the rms

scatter σ_ℓ; (b) average number $\bar{n}$ of glowing centers per unit track length (projection A) and σ_n; (c) logarithmic image density $\bar{D}$, characterizing the brightness of the track and determined by photometry of the streamer tracks with the aid of an MF-4 microphotometer [3].

E, MeV	I/I_{min}	Measured quantity	Measurement series I	II	III
660	1.2	$\bar{n}$	4.35±0.6	5.0±0.6	6.5±0.4
		$\bar{\ell}$	6.0 ±0.8	7.3 ±1.0	11.8±1.1
		$\bar{D}$	0.09±0.03	0.14±0.03	0.23±0.03
		$\sigma_D/\bar{D}$	27%	26%	25%
106	3.4	$\bar{n}$	5.9 ± 0.8	5.8 ± 0.7	–
		$\bar{\ell}$	9.5 ± 1.1	9.3 ± 1.3	14.7 ± 1.5
		$\bar{D}$	0.22 ± 0.05	0.23 ± 0.05	0.52 ± 0.07
		$\sigma_D/\bar{D}$	30%	29%	24%
57	5.4	$\bar{n}$	6.9 ± 0.75	6.3 ± 0.6	–
		$\bar{\ell}$	9.5 ± 1.2	11.2 ± 1.5	15.6 ± 1.9
		$\bar{D}$	0.25 ± 0.07	0.33 ± 0.04	0.80 ± 0.08
		$\sigma_D/\bar{D}$	22%	22%	14%
47	6.3	$\bar{n}$	7.3 ± 0.6	7.7 ± 1.0	–
		$\bar{\ell}$	10.0 ± 1.3	11.7 ± 2.2	18.1 ± 2.2
		$\bar{D}$	0.29 ± 0.06	0.37 ± 0.06	0.80 ± 0.05
		$\sigma_D/\bar{D}$	37%	13%	16%
33	8.5	$\bar{n}$	–	–	–
		$\bar{\ell}$	–	–	22.0 ± 3.8
		$\bar{D}$	–	–	1.15±0.16

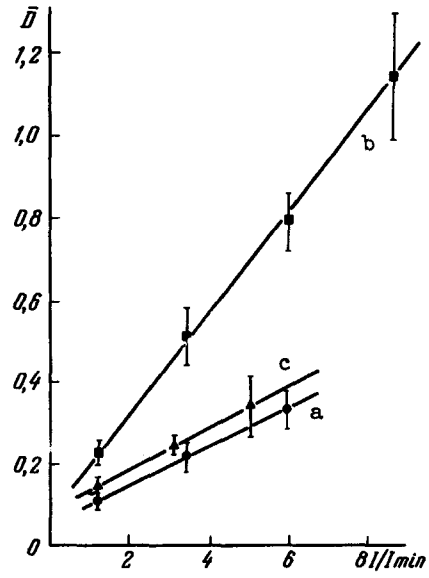

Fig. 2. Calibration plots of D vs. I/I_{min} at high-voltage pulse durations $\bar{\tau}$ (a), τ_{III} (b), and τ_{II} (c). ● - neon, 1 atm; ■ - neon, 1 atm; ▲ - helium, 1 atm.

The measured values of $\bar{n}$, $\bar{\ell}$, and $\bar{D}$ are listed in the table. The errors correspond to one standard deviation. The accuracy with which $\bar{D}$ was determined for any one track, determined for a large number of tracks, is listed in the table in the form of the rms error $\sigma_D/\bar{D}$.

Figure 2 shows calibration plots of the logarithmic-density parameter D against the specific ionization. Plot a was obtained by averaging the results of measurement series I and II, and corresponds to the average duration of the high-voltage pulse, $\bar{\tau} = (\tau_I + \tau_{II})/2$. It is seen from these curves that the dependence of D on I/I_{min} has a character that varies with the duration of the high-voltage pulse. This is evidently connected with the fact that the brightness increases all the faster with the length of the streamer column. The character of the plot of D vs. I/I_{min} obtained for helium is similar to that obtained with neon. However, to obtain the optimal dependence of D in I/I_{min} it is necessary to operate the chamber at a high excess voltage.

By photometrically measuring the frames of stereo pairs of proton-track photographs obtained at different lens apertures, we were able to determine the contrast coefficient γ of the emulsions for our range of densities. This has made it possible obtain a more rigorous

conversion from density to brightness (Fig. 3) than that of our earlier paper [4].

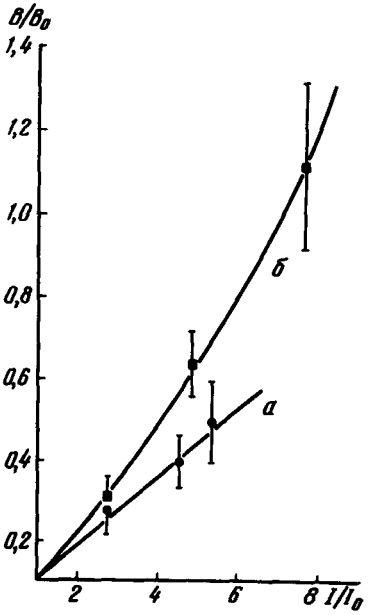

Fig. 3. Relative brightnesses of the proton tracks, B/B_0 (B_0 - average brightness of tracks with ionization $I_0 = 1.2\ I_{min}$) at pulse durations τ and τ_{III}.

In conclusion, the authors thank A. I. Alikhanyan, I. M. Vasilevskii, A. F.Pisarev, A. A. Tyapkin, and G. E. Chikovani for interest, collaboration, and useful discussions, and also A. F. Filozov and R. O. Sharkhatunyan for direct help in performing the experiment and reducing the material.

[1] E. Gygi and F. Schneider, Preprint CERN AR/Int, GS/65-1.
[2] G. E. Chikovani, V. N. Roinishvili, and V. A. Mikhailov, Communications (Soobshcheniya), Georgian Academy of Sciences, 35, 539 (1964).
[3] E. K. Bjornerud, Rev. Sci. Instr. 26, No. 9, (1955).
[4] T. L. Asatiani, K. A. Gazarian, V. N. Zhmirov, E. M. Matevosian, A. A. Nazarian, and R. O. Sharkhatunian, Preprint E-2324, JINR, Dubna, 1965.
*The photograph (Fig.1) was left out of the original Russian issue - Transl.

ERRATA

Vol. 6, No. 4. The following photographs were left out of the earlier edition of the Russian original and were not included in the translated version:

Article by T. L. Asatiani et al, (p. 83):

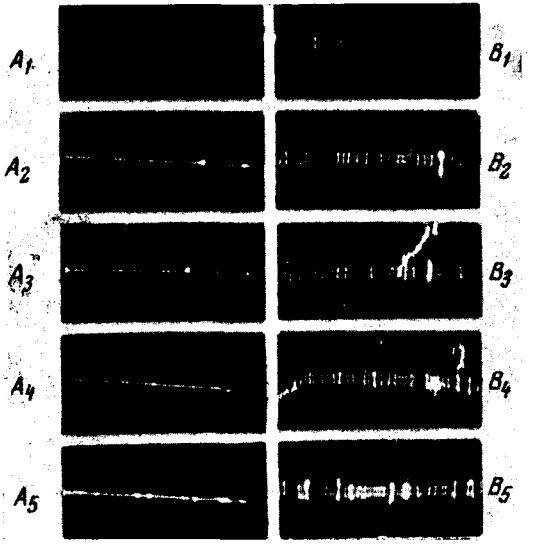

Fig. 1. Photographs of proton tracks in two projections at different energies in the case of a high-voltage pulse duration τ_{III}: A_1, B_1 - $I/I_{min} = 1.2$; A_2, B_2 - $I/I_{min} = 3.4$; A_3, B_3 - $I/I_{min} = 5.4$; A_4, B_4 - $I/I_{min} = 6.3$; A_5, B_5 - $I/I_{min} = 8.5$.

Article by S. A. Akhmanov et al. (p. 85):

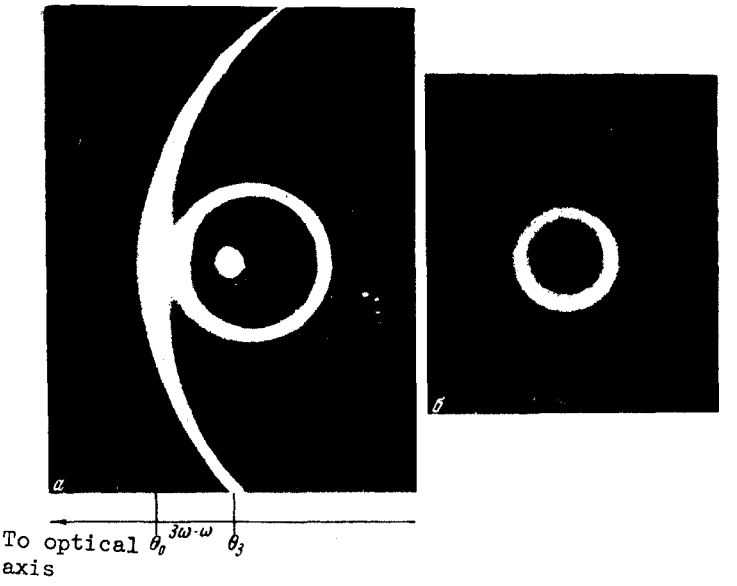

Fig. 2. Space structure in far field: a - emission at difference wavelength $\lambda_2 = 0.53$ μ obtained by mixing the pump and signal at $\lambda_1 = 1.06$ μ (bright spot, ring, and arc) and spontaneous noise (background); b - spontaneous noise passed through interference filter at $\lambda = 5570 \pm 25$ Å; photograph obtained by successive superposition on a single frame of photographs taken at $\theta_3 = \theta_0^{3\omega-\omega} + 5°20'$ (outer ring), $\theta_3 = \theta_0^{3\omega-\omega} + 4°20'$, and $\theta_3 = \theta_0^{3\omega-\omega} + 4°00'$ (two rings coalescing into a single internal one).

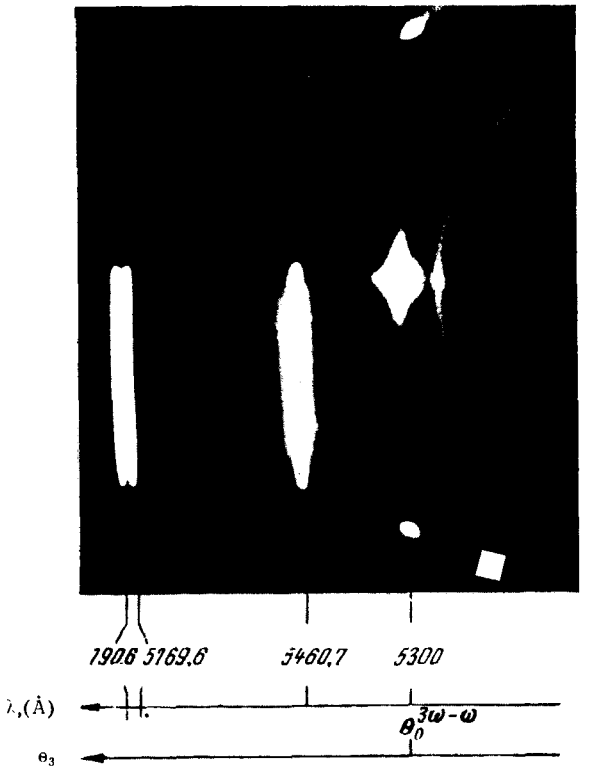

Fig. 3. Spectrograms of spontaneous noise, obtained by superimposing on one frame three spectrograms obtained at angles $\theta_3 - \theta_0^{3\omega-\omega}$ equal to 6°30' (a), 2°55' (b), and 0°35' (c) (arcs from left to right). The reference lines were obtained with a mercury lamp.

Article by V. A. Atsarkin et al. (p. 88):

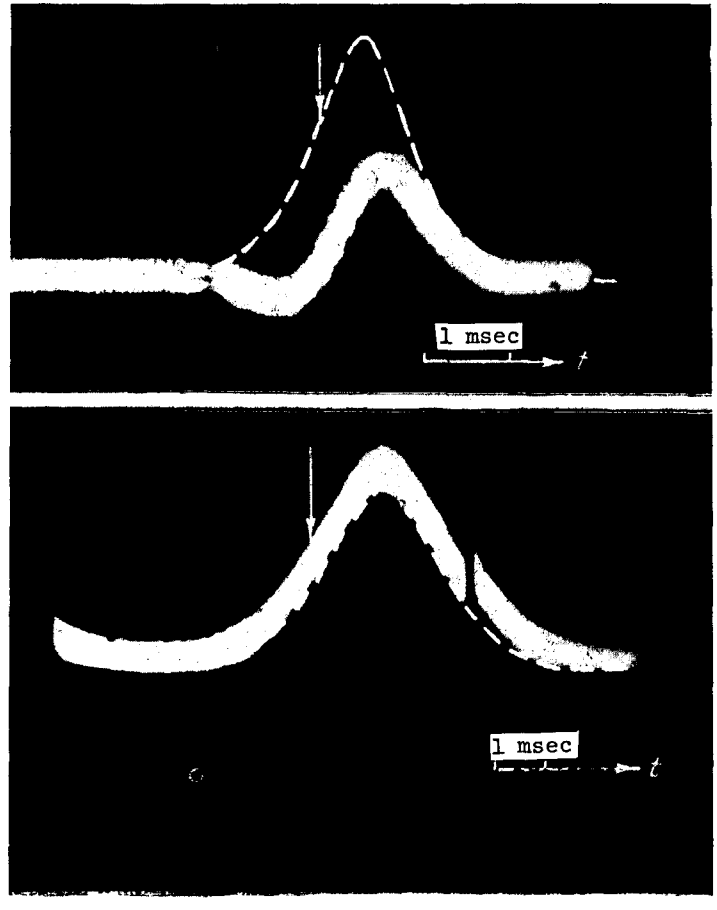

Fig. 2. Oscillograms of EPR line at not-strictly resonant saturation. The notation is the same as in Fig. 1. The magnetic field increases with time in the upper figure and decreases in the lower figure.